

**GEOSAT Sea Level Anomalies in the Western Equatorial Pacific
during the 1986-87 El Nino,
Elucidated as Equatorial Kelvin and Rossby Waves**

Thierry DELCROIX, Gérard ELDIN and Joël PICAUT

*Groupe SURTROPAC, ORSTOM BP A5,
Nouméa - New Caledonia*

ABSTRACT

Thanks to the GEOSAT altimeter data set, information on sea level changes during the 1986-87 El Nino is presented. Special emphasis is placed on the warm pool area, with an evaluation, a detailed description and tentative explanation of the observed Sea Level Anomaly (SLA) changes.

Near the 165°E longitude, the onset of the 1986-87 El Nino is characterized by a rapid development of a positive (>14 cm) equatorial SLA in November/December 1986. This feature occurs in response to an eastward wind anomaly appearing between 140°E-170°W along the equator. The wind induces a downwelling equatorial Kelvin wave with phase speed of about 2.3 m.s⁻¹. Thereafter, equatorial SLA remains quite constant from January to April/May 1987. In June 1987, equatorial SLA decreases to a minimum value, just after an abrupt change of the zonal wind stress anomaly, west of 165°E. Such anomaly seems to force an upwelling equatorial Kelvin wave propagating at about 2.3 m.s⁻¹. Two patches of negative SLAs then appear in September 1987 at 4°N and 4°S, symmetrical about the equator. These are the signature of a first baroclinic upwelling equatorial Rossby wave ($n=l=1$) arising from the eastern boundary, at $c = 0.9$ m.s⁻¹ phase speed. These calculations suggest that first baroclinic mode Kelvin waves and Rossby wave were the dominant sources of sea level changes in the equatorial band, over the November 1986-November 1987 El Nino period.

1. Introduction.

Before 1985, large scale monitoring of the tropical Pacific Ocean relied on island sea level and/or XBT networks. Both monitoring approaches were quite successful in describing and understanding the main tropical Pacific Ocean variability (e.g., Wyrki, 1985; White et al., 1985). However, these observations were respectively limited by the poor spatial coverage of the islands, especially in the eastern Pacific, and the poor temporal resolution of XBT measurements which were also restricted to commercial shipping routes.

The U.S. Navy GEOSAT (GEOdetic SATellite) was launched in March 1985, which coincided with the beginning of the international TOGA programme. Hence, the 1986-87 El Nino phenomenon was the first to be captured by a satellite altimeter, providing unprecedented spatial and temporal resolutions of the tropical Pacific ocean surface variability.

Previous works (Cheney and Miller, 1988; Miller et al., 1988; Tai et al., 1989) have already demonstrated the usefulness of GEOSAT in monitoring the whole tropical Pacific ocean. As a complement, the goal of this note is to specifically focus upon the Sea Level Anomalies (SLAs) measured in the tropical Pacific warm pool during the 1986-87 El Nino. To this end, we first briefly present the GEOSAT data and data processing, then give a description of the SLAs observed in the "center" of the warm pool (165°E longitude), and finally try to understand the origin of the altimeter-derived SLAs.



F 30213

2. Data

a. Data processing.

Detailed information about the GEOSAT mission may be found in a review released by the Applied Physics Laboratory of the Johns Hopkins University (APL, 1987). It is worth reiterating here that the GEOSAT spacecraft was originally launched into a non repeat orbit (March 12, 1985), and then put into a 17-day repeat/collinear orbit configuration (November 18, 1987), for oceanographic applications. Only part of that phase of the mission, referred to as the Exact Repeat Mission (ERM), will be considered here.

The GEOSAT data we have analysed were kindly provided by C. Koblinsky (NASA, Greenbelt). All environmental corrections, e.g. water vapour derived from the Fleet Numerical Oceanographic Center's 12-hour model, were already included. The Sea Level Anomalies (SLAs) data we received, stem from the first year of the ERM; SLAs are thus relative to the mean of the November 1986–November 1987 period. The data consist of 22 grids of SLAs, and figure 1 shows the ground tracks of such a grid over the tropical Pacific ocean. Tracks are separated from each other by about 1.5° at the equator, and there is a measurement every about 7 km along each track.

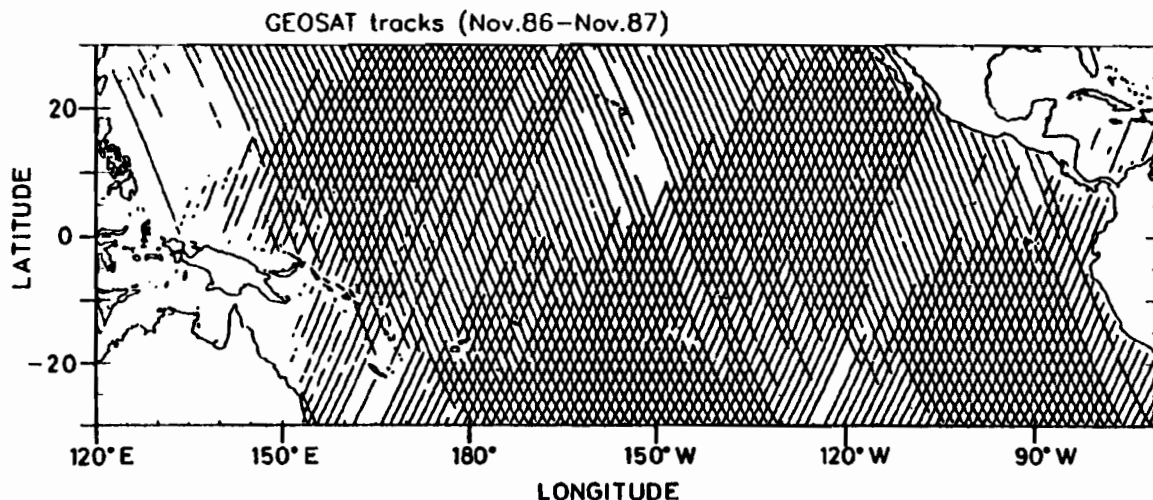


FIG.1. Ground tracks of the GEOSAT 17-day collinear orbit over the tropical Pacific ocean.

Our own data processing was made in three steps. Firstly, along track SLAs were smoothed using 300 km width non-linear median and linear Hanning filters. An example of such processing is given in figure 2. Secondly, by combining several tracks (6-7) in the zonal direction, time series of SLAs were generated in $0.5^\circ \times 10^\circ$ latitude-longitude boxes. Finally, smoothed records were produced by low-pass filtering in time and latitude using a 31-day and 3° -latitude Hanning filters. No smoothing in longitude was performed.

b. Evaluation

Comparisons between GEOSAT sea level and data from tide gauges, inverted echo sounders, and thermistor chains at various locations throughout the Pacific have suggested that altimeter time series have an RMS accuracy of about 3 cm (Cheney et al., 1988). As an example of our intercomparison figure 3 shows a GEOSAT SLA time series obtained in the warm pool (2°S - 165°E), together with the 0/300db dynamic height anomaly derived from the ATLAS thermistor chain mooring at 2°S - 165°E , and the 0/500db dynamic height anomaly obtained from CTD stations made during seven cruises. Although the data may differ by as much as 5 to 12 cm, they generally agree within a few centimeters. Notable

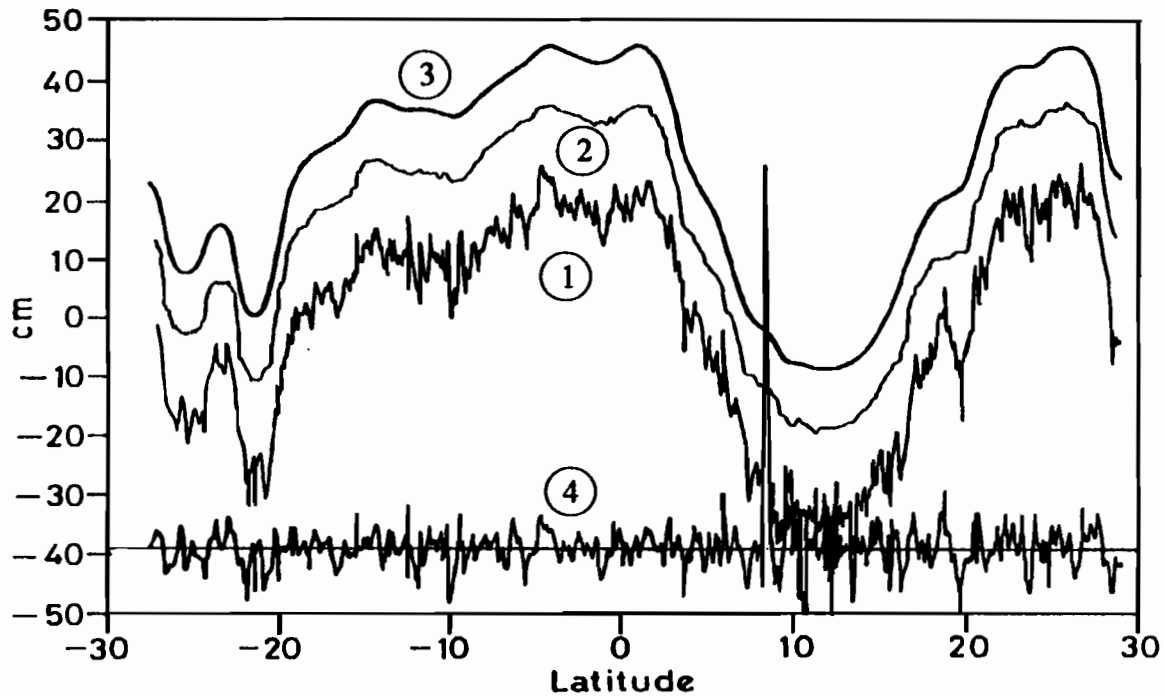


FIG.2. Along track processing of meridional sea level anomalies. Curve 1 denotes the raw sea level anomaly (cm) from 30°S to 30°N. Curve 2 is curve 1 shifted by +10 cm and despiked with a 3°-latitude non-linear median filter. Curve 3 is curve 2 shifted by +10 cm and smoothed with a 3°-latitude Hanning filter. Curve 4 is curve 1 minus curve 3.

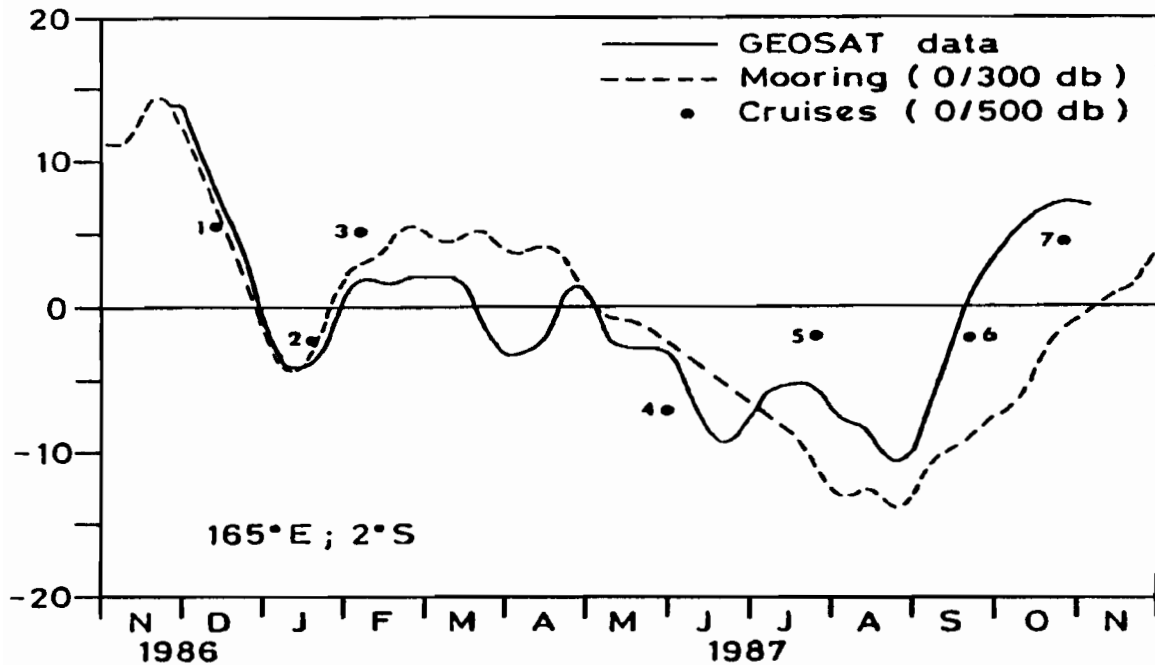


FIG.3. Comparison between Geosat SLA time series (full line), 0/300db dynamic height anomaly time series obtained from ATLAS thermistor chain moorings (broken line), and spot 0/500db dynamic height anomaly measurements derived from CTD stations from seven different cruises. Note that the 0/300 db data were linearly interpolated from May 20 to July 21, 1987. Cruise numbers are (1) US/PRC-2, (2) SURTROPAC-7, (3) JENEX-1, (4) SAGA-2, (5) SURTROPAC-8, (6) PROPPAC-1, and (7) US/PRC-3. The vertical scale denotes either cm (GEOSAT data) or dyn.cm (mooring and cruises).

differences between time series may be due to incomplete correction of environmental errors and/or they may reflect the idiosyncrasies of each type of observations (e.g., the dynamic height time series do not include the variability below 300 db as well as the salinity effects upon dynamic height computation; the CTD stations represent only spot measurements, etc...). The RMS scatter about the fitted line between the altimeter SLAs and the 0/300 db dynamic height anomaly is 4 cm. Thus, based on previous evaluations and on this last comparison, we conclude that GEOSAT altimeter data seems adequate for monitoring sea level variations in the tropics with an RMS accuracy of 4 cm. As a consequence, only SLAs above ± 8 cm, corresponding to a signal/noise = 2, will be further considered.

3. Results

Figure 4 represents the SLAs along the 165°E longitude, as a function of time and latitude. Four patches of SLA above ± 8 cm appear in the equatorial band. Our purpose is to sequentially analyse the mechanisms that generated these patches. In support of this analysis, we will refer to figures 5a-b presenting the zonal wind stress anomaly and SLA along the equator, both as a function of time, from the western to the eastern Pacific.

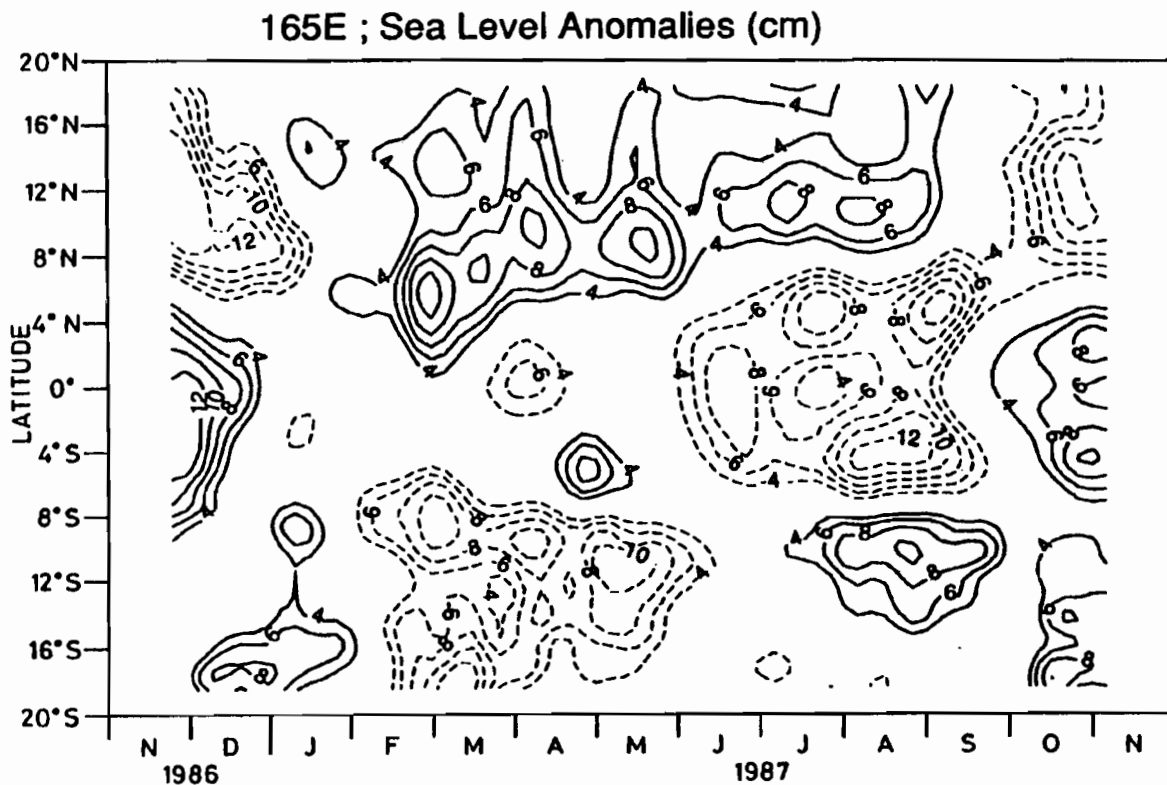


FIG.4. Geosat sea level anomalies (cm) as a function of time and latitude, along the 165°E longitude.

The first significant patch of SLA appears in November/December 1986 (Fig.5b). It occurs in response to eastward wind anomaly located west of about 170°W (Fig.5a). The wind induces a downwelling equatorial Kelvin wave which propagates across the entire basin at about the first baroclinic phase speed $c^k_1 = 2.3 \text{ m.s}^{-1}$ (Eriksen, 1982), as already documented by Miller et al. (1988). A Gaussian fit of the meridional SLA structure, east of the forcing area, is clearly in excellent agreement with the data, within $\pm 5^\circ$ of the equator using $c^k_1 = 2.3 \text{ m.s}^{-1}$ (Fig.6).

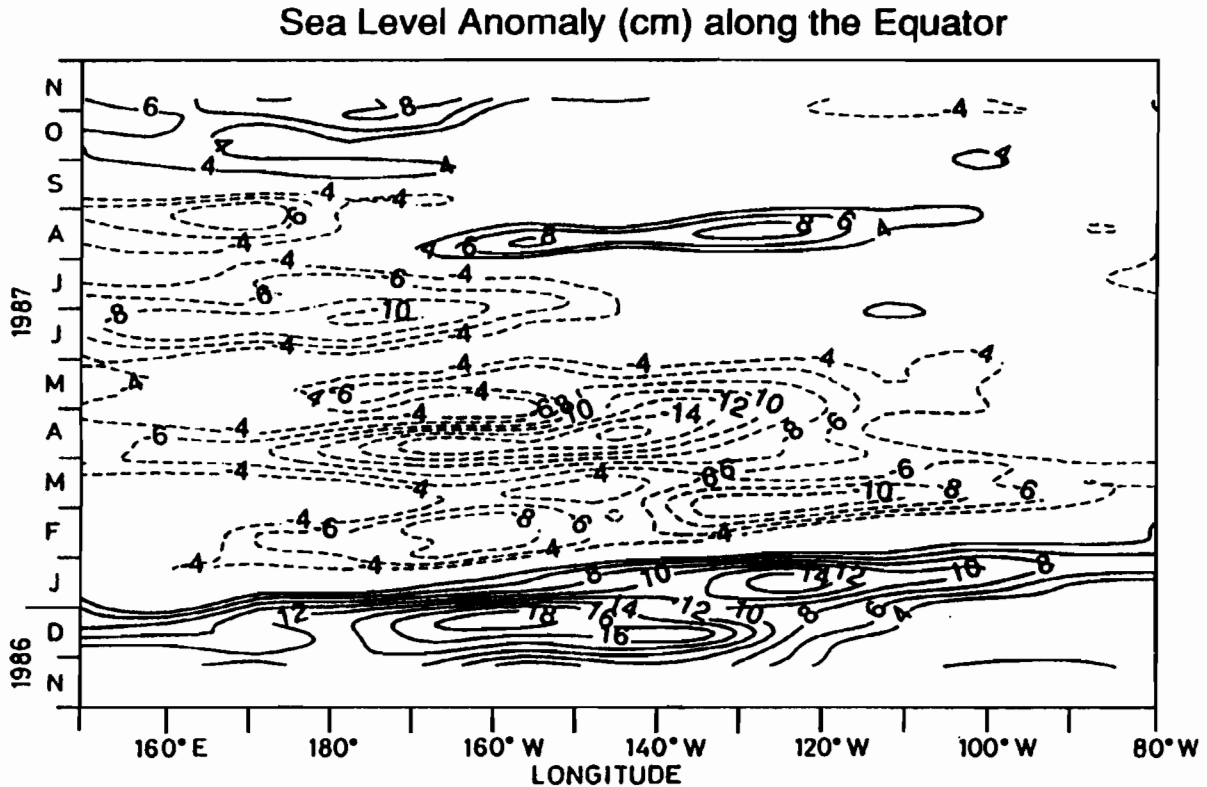
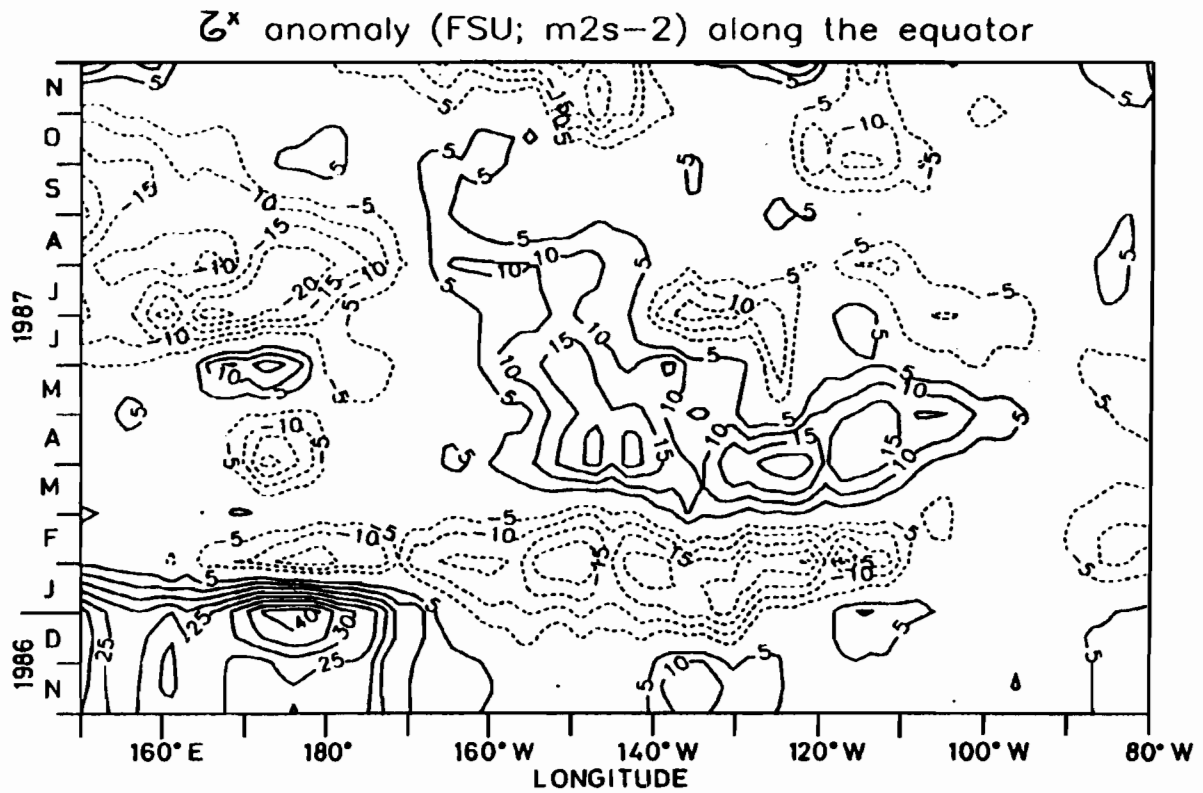


FIG.5. Top (a): Zonal wind stress anomaly ($m^2.s^{-2}$) along the equator as a function of time and longitude; Bottom (b): Sea level anomaly (cm) along the equator as a function of time and longitude.

The second significant sea level signal emerges in June 1987 (Fig.5b), just after a rapid zonal wind stress change near the 165°E longitude (Fig.5a). The wind seems to generate an upwelling Kelvin wave (Fig.5b) that propagates at least to the middle of the basin, where the Kelvin wave meets a downwelling-favorable wind stress. Figure 7 shows that a Gaussian fit of the meridional SLA structure, east of the forcing area, corresponds quite well to the data, within $\pm 5^\circ$ of the equator, using $c^k_1=2.3 \text{ m.s}^{-1}$.

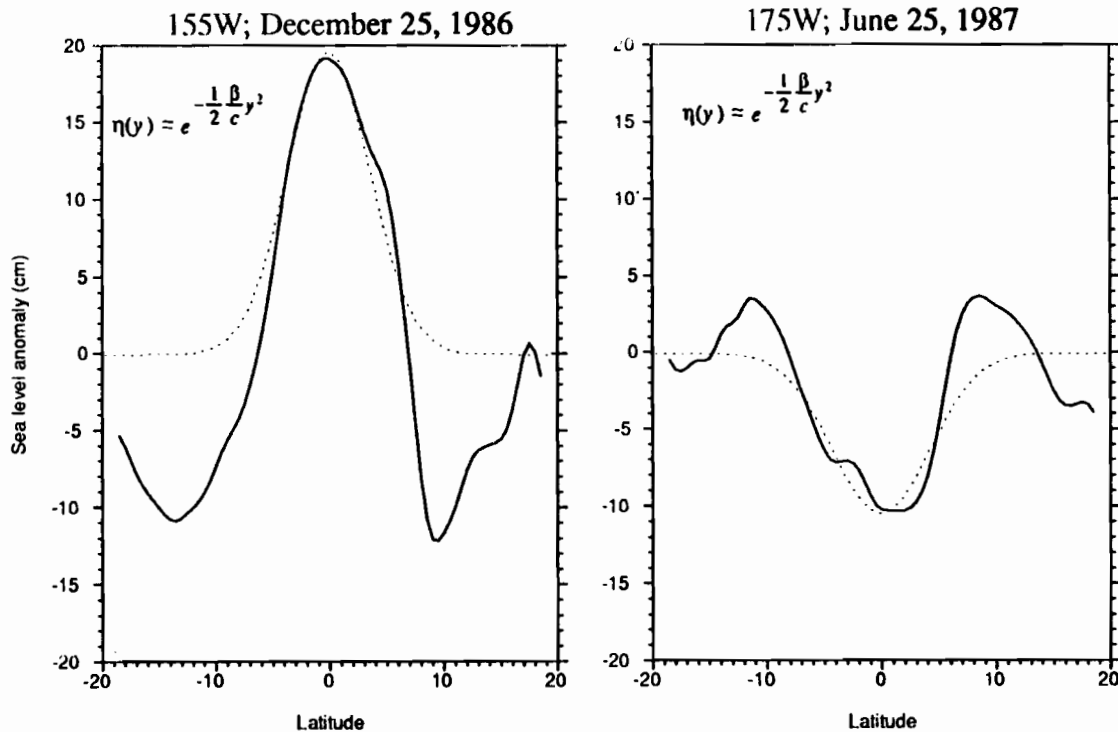


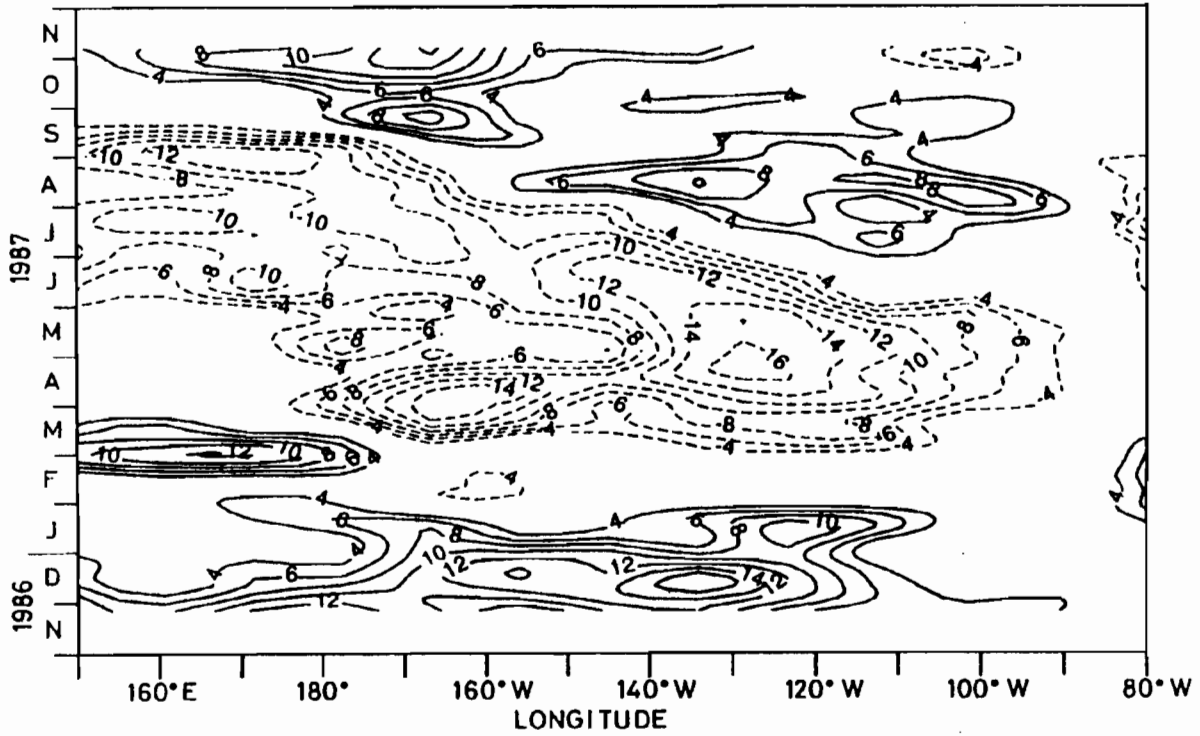
FIG.6. Gaussian fit (broken line) of the meridional (20°S-20°N) sea level anomaly structure (full line) at 155°W longitude, on December 25, 1986.

FIG.7. Gaussian fit (broken line) of the meridional (20°S-20°N) sea level anomaly structure (full line) at 175°W longitude, on June 25, 1987.

Two patches of SLAs in excess of $\pm 8 \text{ cm}$ then arise in August-September 1987, at 165°E, symmetrical about the equator at about 4°N and 4°S (Fig.4). They result from the westward propagation of a first baroclinic ($n=1$) first horizontal ($l=1$) Rossby wave, as shown in Figure 8. The Rossby wave propagates at about $c^R_1=0.9 \text{ m.s}^{-1}$, i.e. about one third ($2l+1=3$) of the aforementioned Kelvin wave phase speed. Figure 10 shows the good agreement between the meridional SLA structure and the theoretical shape of the Rossby wave ($n=l=1$), involving Gaussian and Hermite functions.

The upwelling Rossby wave portrayed in Figure 8 may result from two different mechanisms. First, due to the excellent timing agreement, we suggest that it might be the reflection of the upwelling equatorial Kelvin wave generated by the fast zonal wind stress change occurring east of 165°E, by the end of January 1987 (Fig.5a). This upwelling equatorial Kelvin wave, evidenced in figure 5b, hits the eastern coast by the end of March 1987, and then might reflect as an equatorial upwelling Rossby wave (Fig.8). Second, it should be noted that the upwelling Rossby wave may also be amplified or eventually generated by local forcing, as exemplified in figure 9 which shows a positive Ekman pumping anomaly beginning in early March 1987, between about 100°W and 160°W.

Sea Level Anomaly (cm) along 4N latitude



Sea Level Anomaly (cm) along 4S latitude

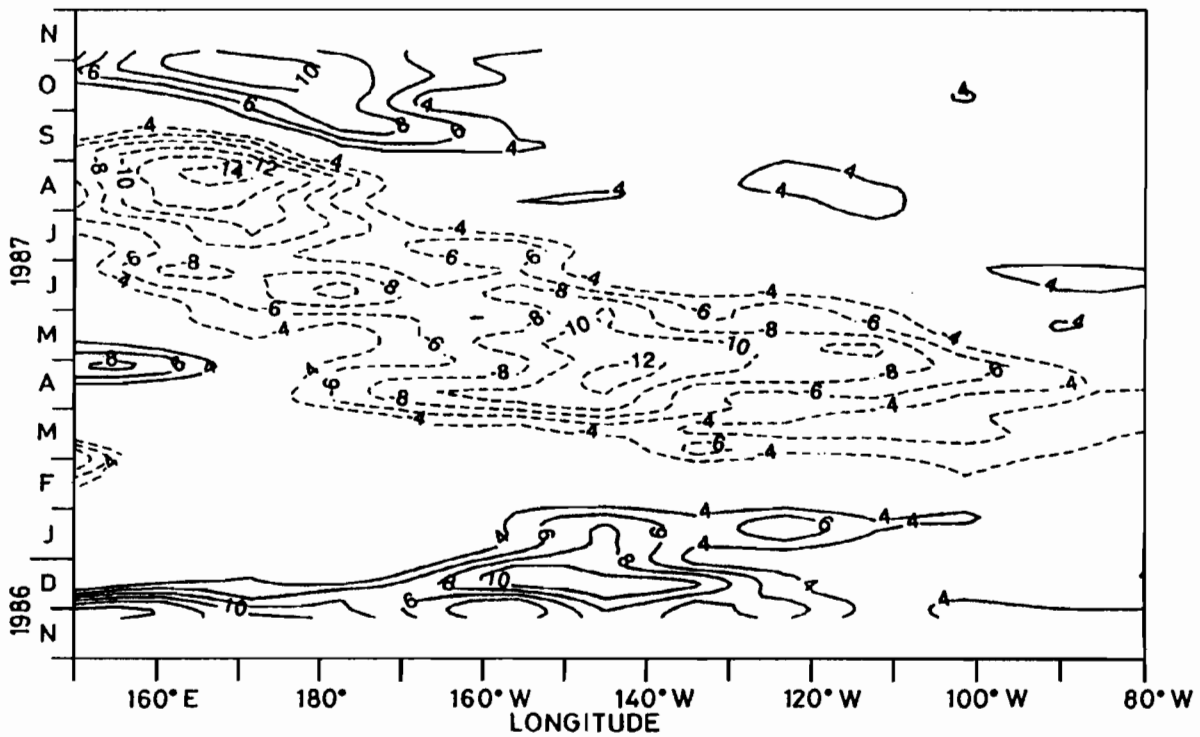
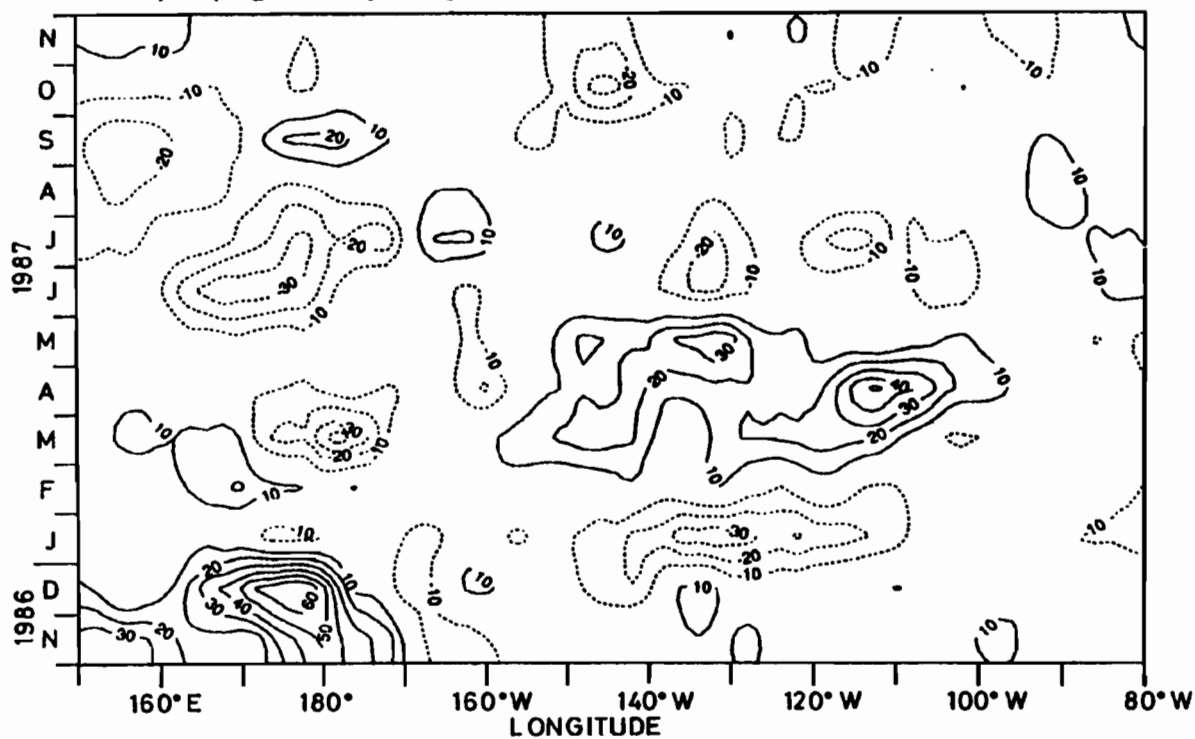


FIG.8. Sea level anomaly (cm) along the 4°N (top panel) and 4°S (bottom panel) latitudes, as a function of time and longitude.

Ekman pumping anomaly along 4N latitude (m/month).



Ekman pumping anomaly along 4S latitude (m/month).

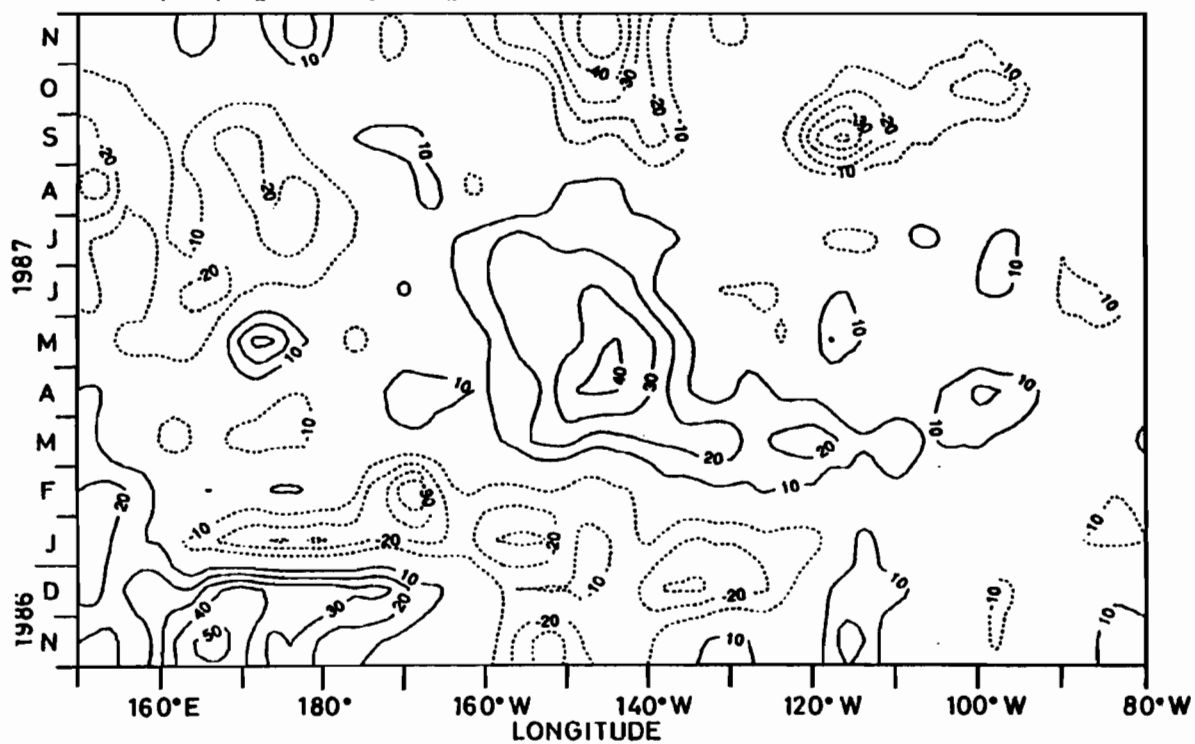


FIG.9. Ekman pumping anomaly ($\text{m}\cdot\text{month}^{-1}$) along the 4°N (top panel) and 4°S (bottom panel) latitudes, as a function of time and longitude. Positive value is upward motion.

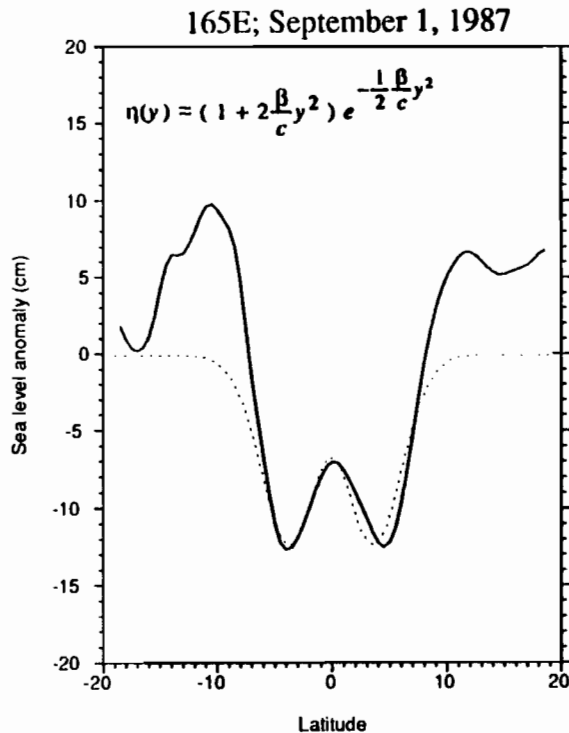


FIG.10. Least square fit (broken line) of the meridional (20°S-20°N) sea level anomaly structure (full line) at 165°E longitude, on September 1, 1987.

The relative importance of both mechanisms is now part of an ongoing study involving linear numerical model results.

In conclusion, we believe that first baroclinic Kelvin waves and ($n=1$) Rossby wave are the dominant sources of sea level changes in the equatorial band, during the 1986-87 El Nino.

Acknowledgements. Fruitful discussions with Yves du Penhoat have been much appreciated. This work could not have been conducted without the GEOSAT data provided by Chet Koblinsky and the programming support of François Masia. Support for this work, as part of the TOPEX/POSEIDON Science Working Team, was provided by the "Programme Télédetection Spatiale", through AIP 59.88.46 and 9.88.25.

REFERENCES

- APL, 1987: The Navy GEOSAT mission, Johns Hopkins Applied Physics Laboratory, technical digest, vol. 8, No 2, 290 pages. (Johns Hopkins Road, Laurel, MD 20707, USA).
- Cheney R. and L. Miller, 1988: Mapping the 1986-1987 El Nino with GEOSAT data. *EOS*, 69, 754-755.
- Cheney R., B. Douglas and L. Miller, 1988: Evaluation of GEOSAT altimeter data with application to tropical Pacific sea level variability. *J. Geophys. Res.*, 95, 4737-4749.
- Eriksen C., 1982: Equatorial wave vertical modes observed in a western Pacific island array. *J. Phys. Oceanogr.*, 12, 1206-1227.
- Miller L., R. Cheney and B. Douglas, 1988: GEOSAT altimeter observations of Kelvin waves and the 1986-87 El Nino. *Science*, 239, 52-54.

- Tai C.K, W. White and S. Pazan, 1989: Geosat crossover analysis in the tropical Pacific. 2. Verification of altimetric sea level maps with XBT and island sea level data. *J. Geophys. Res.*, **94**, 897-908.
- White W., G. Meyers, J.R. Donguy and S. Pazan, 1985: Short term variability in the thermal structure of the Pacific ocean during 1979-82. *J. Phys. Oceanogr.*, **15**, 917-935.
- Wyrski, 1985: Water displacements in the Pacific and the genesis of El Nino cycles. *J. Geophys. Res.*, **90**, 7129-7132.

**WESTERN PACIFIC INTERNATIONAL MEETING
AND WORKSHOP ON TOGA COARE**

**Nouméa, New Caledonia
May 24-30, 1989**

PROCEEDINGS

edited by

Joël Picaut *
Roger Lukas **
Thierry Delcroix *

* ORSTOM, Nouméa, New Caledonia
** JIMAR, University of Hawaii, U.S.A.

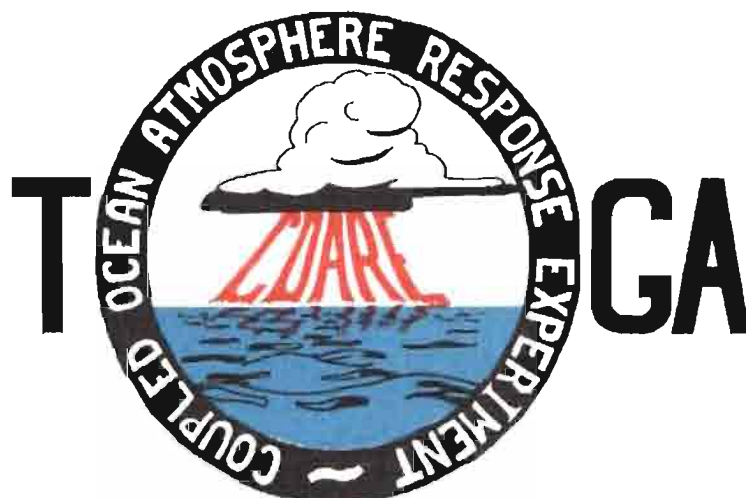


TABLE OF CONTENTS

ABSTRACT	i
RESUME	iii
ACKNOWLEDGMENTS	vi
INTRODUCTION	
1. Motivation	1
2. Structure	2
LIST OF PARTICIPANTS	5
AGENDA	7
WORKSHOP REPORT	
1. Introduction	19
2. Working group discussions, recommendations, and plans	20
a. Air-Sea Fluxes and Boundary Layer Processes	20
b. Regional Scale Atmospheric Circulation and Waves	24
c. Regional Scale Oceanic Circulation and Waves	30
3. Related programs	35
a. NASA Ocean Processes and Satellite Missions	35
b. Tropical Rainfall Measuring Mission	37
c. Typhoon Motion Program	39
d. World Ocean Circulation Experiment	39
4. Presentations on related technology	40
5. National reports	40
6. Meeting of the International Ad Hoc Committee on TOGA COARE	40
APPENDIX: WORKSHOP RELATED PAPERS	
Robert A. Weller and David S. Hosom: Improved Meteorological Measurements from Buoys and Ships for the World Ocean Circulation Experiment	45
Peter H. Hildebrand: Flux Measurement using Aircraft and Radars	57
Walter F. Dabberdt, Hale Cole, K. Gage, W. Ecklund and W.L. Smith: Determination of Boundary-Layer Fluxes with an Integrated Sounding System	81

MEETING COLLECTED PAPERS

WATER MASSES, SEA SURFACE TOPOGRAPHY, AND CIRCULATION

Klaus Wyrtki: Some Thoughts about the West Pacific Warm Pool	99
Jean René Donguy, Gary Meyers, and Eric Lindstrom: Comparison of the Results of two West Pacific Oceanographic Expeditions FOC (1971) and WEPOCS (1985-86)	111
Dunxin Hu, and Maochang Cui: The Western Boundary Current in the Far Western Pacific Ocean	123
Peter Hacker, Eric Firing, Roger Lukas, Philipp L. Richardson, and Curtis A. Collins: Observations of the Low-latitude Western Boundary Circulation in the Pacific during WEPOCS III	135
Stephen P. Murray, John Kindle, Dharma Arief, and Harley Hurlburt: Comparison of Observations and Numerical Model Results in the Indonesian Throughflow Region	145
Christian Henin: Thermohaline Structure Variability along 165°E in the Western Tropical Pacific Ocean (January 1984 - January 1989)	155
David J. Webb, and Brian A. King: Preliminary Results from Charles Darwin Cruise 34A in the Western Equatorial Pacific	165
Warren B. White, Nicholas Graham, and Chang-Kou Tai: Reflection of Annual Rossby Waves at The Maritime Western Boundary of the Tropical Pacific	173
William S. Kessler: Observations of Long Rossby Waves in the Northern Tropical Pacific	185
Eric Firing, and Jiang Songnian: Variable Currents in the Western Pacific Measured During the US/PRC Bilateral Air-Sea Interaction Program and WEPOCS	205
John S. Godfrey, and A. Weaver: Why are there Such Strong Steric Height Gradients off Western Australia ?	215
John M. Toole, R.C. Millard, Z. Wang, and S. Pu: Observations of the Pacific North Equatorial Current Bifurcation at the Philippine Coast	223

EL NINO/SOUTHERN OSCILLATION 1986-87

Gary Meyers, Rick Bailey, Eric Lindstrom, and Helen Phillips: Air/Sea Interaction in the Western Tropical Pacific Ocean during 1982/83 and 1986/87	229
Laury Miller, and Robert Cheney: GEOSAT Observations of Sea Level in the Tropical Pacific and Indian Oceans during the 1986-87 El Nino Event	247
Thierry Delcroix, Gérard Eldin, and Joël Picaut: GEOSAT Sea Level Anomalies in the Western Equatorial Pacific during the 1986-87 El Nino, Elucidated as Equatorial Kelvin and Rossby Waves	259
Gérard Eldin, and Thierry Delcroix: Vertical Thermal Structure Variability along 165°E during the 1986-87 ENSO Event	269
Michael J. McPhaden: On the Relationship between Winds and Upper Ocean Temperature Variability in the Western Equatorial Pacific	283

John S. Godfrey, K. Ridgway, Gary Meyers, and Rick Bailey: Sea Level and Thermal Response to the 1986-87 ENSO Event in the Far Western Pacific	291
Joël Picaut, Bruno Camusat, Thierry Delcroix, Michael J. McPhaden, and Antonio J. Busalacchi: Surface Equatorial Flow Anomalies in the Pacific Ocean during the 1986-87 ENSO using GEOSAT Altimeter Data	301

THEORETICAL AND MODELING STUDIES OF ENSO AND RELATED PROCESSES

Julian P. McCreary, Jr.: An Overview of Coupled Ocean-Atmosphere Models of El Nino and the Southern Oscillation	313
Kensuke Takeuchi: On Warm Rossby Waves and their Relations to ENSO Events	329
Yves du Penhoat, and Mark A. Cane: Effect of Low Latitude Western Boundary Gaps on the Reflection of Equatorial Motions	335
Harley Hurlburt, John Kindle, E. Joseph Metzger, and Alan Wallcraft: Results from a Global Ocean Model in the Western Tropical Pacific	343
John C. Kindle, Harley E. Hurlburt, and E. Joseph Metzger: On the Seasonal and Interannual Variability of the Pacific to Indian Ocean Throughflow	355
Antonio J. Busalacchi, Michael J. McPhaden, Joël Picaut, and Scott Springer: Uncertainties in Tropical Pacific Ocean Simulations: The Seasonal and Interannual Sea Level Response to Three Analyses of the Surface Wind Field	367
Stephen E. Zebiak: Intraseasonal Variability - A Critical Component of ENSO ?	379
Akimasa Sumi: Behavior of Convective Activity over the "Jovian-type" Aqua-Planet Experiments	389
Ka-Ming Lau: Dynamics of Multi-Scale Interactions Relevant to ENSO	397
Pecheng C. Chu and Roland W. Garwood, Jr.: Hydrological Effects on the Air-Ocean Coupled System	407
Sam F. Iacobellis, and Richard C.J. Somerville: A one Dimensional Coupled Air-Sea Model for Diagnostic Studies during TOGA-COARE	419
Allan J. Clarke: On the Reflection and Transmission of Low Frequency Energy at the Irregular Western Pacific Ocean Boundary - a Preliminary Report	423
Roland W. Garwood, Jr., Pecheng C. Chu, Peter Muller, and Niklas Schneider: Equatorial Entrainment Zone : the Diurnal Cycle	435
Peter R. Gent: A New Ocean GCM for Tropical Ocean and ENSO Studies	445
Wasito Hadi, and Nuraini: The Steady State Response of Indonesian Sea to a Steady Wind Field	451
Pedro Ripa: Instability Conditions and Energetics in the Equatorial Pacific	457
Lewis M. Rothstein: Mixed Layer Modelling in the Western Equatorial Pacific Ocean	465
Neville R. Smith: An Oceanic Subsurface Thermal Analysis Scheme with Objective Quality Control	475
Duane E. Stevens, Qi Hu, Graeme Stephens, and David Randall: The hydrological Cycle of the Intraseasonal Oscillation	485
Peter J. Webster, Hai-Ru Chang, and Chidong Zhang: Transmission Characteristics of the Dynamic Response to Episodic Forcing in the Warm Pool Regions of the Tropical Oceans	493

MOMENTUM, HEAT, AND MOISTURE FLUXES BETWEEN ATMOSPHERE AND OCEAN

W. Timothy Liu: An Overview of Bulk Parametrization and Remote Sensing of Latent Heat Flux in the Tropical Ocean	513
E. Frank Bradley, Peter A. Coppin, and John S. Godfrey: Measurements of Heat and Moisture Fluxes from the Western Tropical Pacific Ocean	523
Richard W. Reynolds, and Ants Leetmaa: Evaluation of NMC's Operational Surface Fluxes in the Tropical Pacific	535
Stanley P. Hayes, Michael J. McPhaden, John M. Wallace, and Joël Picaut: The Influence of Sea-Surface Temperature on Surface Wind in the Equatorial Pacific Ocean	543
T.D. Keenan, and Richard E. Carbone: A Preliminary Morphology of Precipitation Systems In Tropical Northern Australia	549
Phillip A. Arkin: Estimation of Large-Scale Oceanic Rainfall for TOGA	561
Catherine Gautier, and Robert Frouin: Surface Radiation Processes in the Tropical Pacific	571
Thierry Delcroix, and Christian Henin: Mechanisms of Subsurface Thermal Structure and Sea Surface Thermo-Haline Variabilities in the South Western Tropical Pacific during 1979-85 - A Preliminary Report	581
Greg. J. Holland, T.D. Keenan, and M.J. Manton: Observations from the Maritime Continent : Darwin, Australia	591
Roger Lukas: Observations of Air-Sea Interactions in the Western Pacific Warm Pool during WEPOCS	599
M. Nunez, and K. Michael: Satellite Derivation of Ocean-Atmosphere Heat Fluxes in a Tropical Environment	611

EMPIRICAL STUDIES OF ENSO AND SHORT-TERM CLIMATE VARIABILITY

Klaus M. Weickmann: Convection and Circulation Anomalies over the Oceanic Warm Pool during 1981-1982	623
Claire Perigaud: Instability Waves in the Tropical Pacific Observed with GEOSAT	637
Ryuichi Kawamura: Intraseasonal and Interannual Modes of Atmosphere-Ocean System Over the Tropical Western Pacific	649
David Gutzler, and Tamara M. Wood: Observed Structure of Convective Anomalies	659
Siri Jodha Khalsa: Remote Sensing of Atmospheric Thermodynamics in the Tropics	665
Bingrong Xu: Some Features of the Western Tropical Pacific: Surface Wind Field and its Influence on the Upper Ocean Thermal Structure	677
Bret A. Mullan: Influence of Southern Oscillation on New Zealand Weather	687
Kenneth S. Gage, Ben Basley, Warner Ecklund, D.A. Carter, and John R. McAfee: Wind Profiler Related Research in the Tropical Pacific	699
John Joseph Bates: Signature of a West Wind Convective Event in SSM/I Data	711
David S. Gutzler: Seasonal and Interannual Variability of the Madden-Julian Oscillation	723
Marie-Hélène Radenac: Fine Structure Variability in the Equatorial Western Pacific Ocean	735
George C. Reid, Kenneth S. Gage, and John R. McAfee: The Climatology of the Western Tropical Pacific: Analysis of the Radiosonde Data Base	741

Chung-Hsiung Sui, and Ka-Ming Lau: Multi-Scale Processes in the Equatorial Western Pacific	747
Stephen E. Zebiak: Diagnostic Studies of Pacific Surface Winds	757

MISCELLANEOUS

Rick J. Bailey, Helene E. Phillips, and Gary Meyers: Relevance to TOGA of Systematic XBT Errors	775
Jean Blanchot, Robert Le Borgne, Aubert Le Bouteiller, and Martine Rodier: ENSO Events and Consequences on Nutrient, Planktonic Biomass, and Production in the Western Tropical Pacific Ocean	785
Yves Dandonneau: Abnormal Bloom of Phytoplankton around 10°N in the Western Pacific during the 1982-83 ENSO	791
Cécile Dupouy: Sea Surface Chlorophyll Concentration in the South Western Tropical Pacific, as seen from NIMBUS Coastal Zone Color Scanner from 1979 to 1984 (New Caledonia and Vanuatu)	803
Michael Szabados, and Darren Wright: Field Evaluation of Real-Time XBT Systems	811
Pierre Rual: For a Better XBT Bathy-Message: Onboard Quality Control, plus a New Data Reduction Method	823